Preprint J. Phys. Soc. Jpn. 83, 084801 (1-6) (2014)

Freeze Dried Zn-DNA: Magnetism Dominated by Water Molecules

Tsubasa Kumeta, Hirokazu Sakamoto*, and Kenji Mizoguchi*

Department of Physics, Tokyo Metropolitan University, Hachioji, Tokyo 192-0397, Japan

Magnetic behaviors in freeze dried DNA complexes with Zn ions (FD-Zn-DNA) are reported. Dehydrated Zn-DNA was prepared from pure Zn-DNA by a freeze drying procedure. Complete dehydration of Zn-DNA by the freeze drying induces an irreversible structural change and produces one π electron spin at each base pair of FD-Zn-DNA. Magnetic behaviors essential to the π electron spins are markedly changed by introducing water molecules in FD-Zn-DNA. In the dehydrated FD-Zn-DNA, the paramagnetism of the π spin system is totally suppressed because of the spin singlet ground state caused by the strong off-site Coulomb repulsion V, which is larger than the on-site Coulomb repulsion U. In contrast, the hydrated FD-Zn-DNA carries large Pauli-like temperature-independent paramagnetism, whose magnitude corresponds to the π-band width of $\approx$ 0.24 eV. A possible mechanism of the π electron spin creation is proposed. As a subsidiary effect of the freeze drying procedure, the nonlinear paramagnetism saturating below 0.1 T is observed in both DNA and Zn-DNA. The nonlinear paramagnetism disappears after the hydration of the sample. On the basis of the magnitude of the saturation magnetization, it is suggested that the origin of the nonlinear paramagnetism is the magnetic impurities in DNA.

1. Introduction

The physical properties of natural deoxyribonucleic acid (DNA) and metal-ion-inserted DNA (M-DNA) have attracted much interest in recent years because of their scientific interest and potential applications to self-assembled nanostructures and nanowires for nanoelectronics.[1–16] Many reports on the electronic properties of natural DNA extracted from λ-phage, calf thymus, and salmon testes showed its diverse nature, namely, it can be insulating,[8] semiconducting,[3,5,10,13] conducting,[1,6,7,11,14] and proximity superconducting.[7] Such diversity would result from salt residues, electron bombardment by an electron microscope, effective doping, *etc.*.[17] It is now commonly known that DNA has semiconducting electronic

*E-mail: sakamoto@phys.se.tmu.ac.jp; mizoguchi@phys.se.tmu.ac.jp

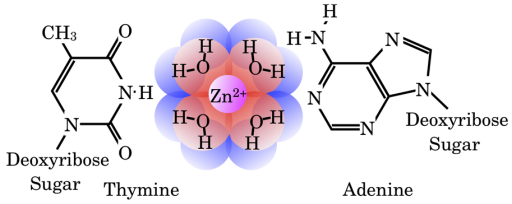

Fig. 1. (Color online) Model of adenine-Zn-thymine in Zn-DNA.[20] The water molecules force the bonding to be ionic, which prevents the Zn ion from forming covalent bonds with the nitrogen atoms of the bases.

states with an energy gap of 4 eV.

Thus, the introduction of charge carriers into the base π-band has been an interesting topic. Divalent metal cations are inserted between each complementary base pair of double helix, adenine-thymine or guanine-cytosine, to modify the electronic states of DNA.[6,10–15,18–21] The resulting DNA complex is called M-DNA, where M is the metal cation. Rakitin *et al*. have reported that Zn-DNA has ohmic *I*-*V* characteristics, which is in sharp contrast with the natural DNA.[6] However, M-DNA with Zn, Ca, Mg, or Mn prepared by the ethanol precipitation does not carry the paramagnetism accompanying the possible charge carrier injection, suggesting that no charge injection was established with the insertion of these divalent metal cations.[10,13–15] This fact indicates that the divalent cations in M-DNA simply replace two sodium cations in Na^+-DNA, keeping the charge balance unchanged. The only exception is Fe-DNA, in which Fe^{2+} is transformed into Fe^{3+}, by injecting one electron into the base π-band.[15,21] In M-DNA synthesized by the ethanol precipitation, the metal cations are hydrated by several water molecules, preventing the cations from forming covalent bonds with the nitrogen atoms of the bases, as described in Fig. 1.[20]

Recently, Omerzu *et al*. have reported a new type of Zn-DNA synthesis by a freeze drying. They applied the freeze drying procedure to a mixture of Zn-DNA, $ZnCl_2$, and tris-HCl buffer solution.[22] The temperature dependence of ESR intensity shows Pauli-like temperature-independent paramagnetism, with which they concluded that the degenerated π electron system had been realized with DNA. They proposed that the charge transfer from the tris-HCl buffer to DNA is the mechanism underlying the observation. This report suggests that the electronic states of Zn-DNA are not unique, but depend on the sample preparation method. Unfortunately, it would be difficult to make the mechanism unambiguously clear with their mixture sample, because the mixture sample is not necessarily suitable for studying the other physical properties. On the basis of our experience so far, we assumed that the removal of water molecules from Zn-DNA by the freeze drying procedure would be an intrinsic mechanism

underlying these findings. Thus, we started this investigation of the mechanism using high-purity Zn-DNA prepared by the ethanol precipitation. Finally, a new model for describing all the present findings is proposed.

2. Experimental

Zn-DNA is prepared with an aqueous solution of 2 mM DNA (salmon sperm DNA, hereafter, called B-DNA) supplied by the Ogata Materials Science Lab. and Sigma-Aldrich and 20 mM $ZnCl_2$ purchased from Wako Pure Chemicals and Sigma-Aldrich. Excess cold ethanol at -20 °C is poured into the transparent DNA-$ZnCl_2$ aqueous solution resulting in a transparent precipitate of Zn-DNA. The residual $ZnCl_2$ is washed out thoroughly from the obtained precipitate with an excess amount of pure ethanol, in which DNA is insoluble. Thus, we obtained pure Zn-DNA without $ZnCl_2$ or any other buffer materials. For the preparation of FD-Zn-DNA, an aqueous solution of Zn-DNA was dripped into a flask at liquid nitrogen temperature and frozen instantly. The flask was immersed in a low-temperature bath down to -15 °C and evacuated with a cold trap for several days to a week. The final product, completely dehydrated FD-Zn-DNA, has a white-colored, polystyrene form. Samples for superconducting quantum interference device (SQUID) susceptometer and ESR were sealed in quartz tubes with He gas for thermal exchange.

3. Discussion

3.1 Magnetic susceptibility

Figure 2 shows SQUID magnetization curves of B-DNA and Zn-DNA at 100 K, prepared by several different procedures. The open diamonds with the solid line show the diamagnetism of B-DNA. The magnetization of Zn-DNA dried in air (Air) is represented by the closed circles, which shows the large DNA diamagnetism with tiny paramagnetism, which was assigned to magnetic impurities.[10] This result is consistent with the previously reported conclusion on the ethanol precipitated M-DNAs, that is, the metal ions maintain divalency with ionic bonds in M-DNA and thus no charge transfer from M to DNA has occurred.[10,15,23–26] An effect of the freeze drying applied to Zn-DNA is demonstrated typically in FD-Zn-A and FD-Zn-B (Fig. 2). FD-Zn-A shows markedly large nonlinear paramagnetism against the magnetic field B with the diamagnetism of Zn-DNA. In contrast, FD-Zn-B has smaller nonlinear paramagnetism, i.e., less than one-third that of FD-Zn-A, and linear paramagnetism in addition to the diamagnetism. Here, we have two characteristic features to discuss concerning the freeze dried Zn-DNA, as follows.

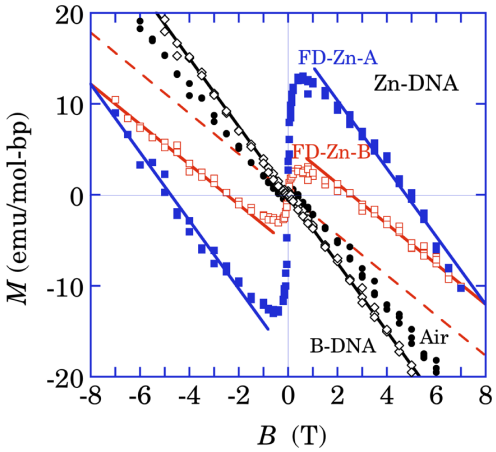

Fig. 2. (Color online) Magnetization per unit containing one base pair of B-DNA and various Zn-DNAs at 100 K, at which oxygen molecules contaminating the data have only a small contribution, as demonstrated in Fig. 3.[13] Open diamonds represent the diamagnetism of as-received salmon DNA (B-DNA). Closed circles show the magnetization of Zn-DNA dried in air ("Air") with large diamagnetism of Zn-DNA and small paramagnetism. FD-Zn-A and FD-Zn-B represent the magnetization of two different batches of the freeze dried Zn-DNA with much larger nonlinear paramagnetism than that of the Zn-DNA dried in air. The solid straight line on FD-Zn-A is almost parallel to the diamagnetism of B-DNA. In contrast, the baseline of FD-Zn-B represented by the dashed line clearly contains the additional linearly increasing paramagnetism with the magnetic field B over the diamagnetism of B-DNA.

(1) Nonlinear paramagnetism in all Zn-DNAs

(2) Linear paramagnetism in FD-Zn-B

Concerning the first point, in the 1960s, strong nonlinear paramagnetism of the freeze dried DNA was observed and extensively studied. Blois Jr. *et al*. concluded on the basis of their experiments and consideration that the submicron ferromagnetic particles tightly attached to the nucleic acid yielded strong nonlinear paramagnetism as a dominant part of ESR signals in DNA.[27] The ferromagnetic particles were originated from the Waring Blendor used in the DNA extraction. In recently available commercial DNA samples, such strong contamination is eliminated. Recently, however, Lee *et al*. have observed a nonlinear paramagnetism at 300 K, especially in B-DNA evacuated for a long term (*without Zn* ions), but with very small amplitude compared with that of FD-Zn-A.[28] They interpreted the nonlinear paramagnetism due to the orbital magnetization of the persistent ring current through mesoscopic DNA loops as the origin of the "S"-shaped M vs B curves.[11] The present data shown in Fig. 2 are, however, reasonably understood from the simple saturating paramagnetism up to 7 T within the uncertainty, as suggested by the straight lines for FD-Zn-A and FD-Zn-B. Another issue for

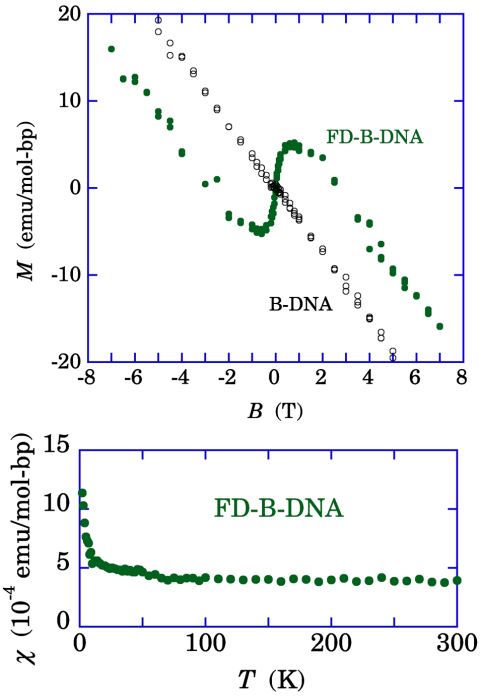

Fig. 3. (Color online) Magnetization at 100 K and susceptibility at 1 T in B-DNA and freeze dried B-DNA. B-DNA shows pure diamagnetism, but the freeze drying treatment at -3°C induces the large nonlinear paramagnetism, which has a comparable magnitude with that of FD-Zn-A and the temperature independent paramagnetism, which mimics Pauli paramagnetism. The upturn below 50 K is caused by oxygen molecules. These features are also observed in the FD-Zn-DNAs, as shown in Fig. 2.

this interpretation is the fact that the saturating magnetization shows only weak temperature dependence up to 300 K, which is difficult to interpret with the quantum mechanical persistent ring current at such high temperatures. By a long-term evacuation of B-DNA at room temperature, we also reproduced a similar magnitude of nonlinear paramagnetism with one-tenth of M_0 of FD-Zn-A. Furthermore, we confirmed by the freeze drying procedure that B-DNA without Zn ions shows large nonlinear paramagnetism comparable to that of FD-Zn-A, as shown in Fig. 3. These facts suggest that the nonlinear paramagnetism emerges in the completely dehydrated DNA as a subsidiary effect of the freeze drying procedure, but is not related to the presence of Zn ions.

One key feature for interpreting the origin of the nonlinear paramagnetism is its magnitude. The magnitude of the nonlinear paramagnetism observed in FD-Zn-A, described as $M_0 = Ng\mu_B S$ in the ferromagnetic case, corresponds to as small as 0.3% of the $S = \frac{1}{2}$ spin or 0.01% of the $S = \frac{5}{2}$ spin per base pair, suggesting an impurity effect. The Fe impurity concentration of $0.1\% - 0.2\%$ per base pair obtained by X-ray fluorescence analysis is con-

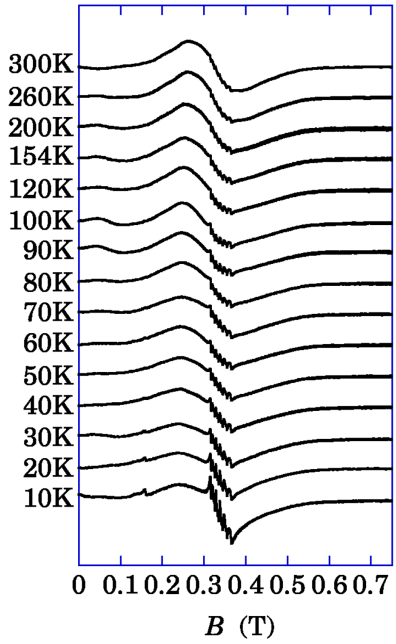

Fig. 4. (Color online) ESR spectra of FD-Zn-A at X-band from 10 to 300 K. The main signal at ≈ 0.326 T ($g \approx 2.1$) corresponds to the nonlinear paramagnetism shown in Fig. 2. The six hyperfine split signals at 0.34 T originate from Mn impurities, which are isolated from each other. Note that the intensity of the isolated Mn signals increases with decreasing temperature following the Curie law, but the broad main signal shows no marked change in its area with temperature. The line width of the main signal is ≈0.1 T at 300 K and gradually increases with decreasing temperature.

sistent with that of a mixture of the high spin states ($S = \frac{5}{2}$) and the low spin states ($S = \frac{1}{2}$). The second point will be discussed in Sec. 3.3 with other new data and with the model for interpreting all the data consistently.

3.2 ESR spectra

The ESR signal of FD-Zn-A at ≈ 0.326 T ($g \approx 2.1$) is shown in Fig. 4. The intensity of the main broad ESR signal is approximately temperature independent. In contrast, the Curie law behavior of the intensity of the six small hyperfine split signals for isolated Mn impurities at 0.3 – 0.36 T is characteristic. The temperature independence of the main ESR signal is apparently consistent with both the nonlinear paramagnetism (bottom panel of Fig. 3) and the Pauli-like paramagnetism. Thus, it is noteworthy that when one interprets the temperature-independent ESR intensity, such as in Fig. 4 and in the report by Omerzu *et al.*,[22] it is impossible to differentiate the Pauli-like paramagnetism from the nonlinear paramagnetism without magnetization data. In contrast, this fact is incompatible with the reported conclusion based on the orbital magnetization of the persistent ring current,[11] which does not give ESR signals

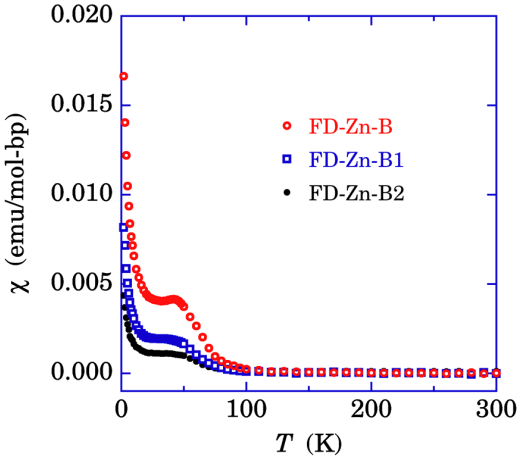

Fig. 5. (Color online) Temperature dependence of the magnetic susceptibility χ of FD-Zn-B, FD-Zn-B1, and FD-Zn-B2 at 1 T. The large bump below 100 K and the Curie-Weiss behavior below 30 K originate from the oxygen molecules trapped in the cells of the freeze dried Zn-DNA. The effect of the mechanical treatment is clearly demonstrated as a reduction of the oxygen contribution below 100 K.

in general.

3.3 Nature of FD-Zn-DNA

3.3.1 Effect of moisture on magnetic properties

The observation of the unique magnetic behavior in the course of sample treatments gave us a crucial insight into the electronic states of FD-Zn-DNA. Freeze dried samples appear to have a polystyrene-like tiny closed cell structure with nanoscale holes for water molecules to exit from the cells. Just after the freeze drying procedure, the closed cells of a sample are almost empty because of the long-term evacuation in the procedure. After that, the sample was transferred to a quartz tube in air, and He gas for thermal exchange was introduced after a short-term evacuation. This procedure in air introduces air contamination into the sample, and the short-term evacuation is insufficient to remove all the oxygen molecules via the nanoscale holes, as confirmed in the χ-T data shown in Fig. 5, which reveals considerable oxygen contamination below 100 K.[13] Thus, we tried to break the closed cells of the sample mechanically, which assists in removing air from the sample with the short-term evacuation.

The evolution of magnetization in FD-Zn-DNA by mechanical treatments is shown in Figs. 5 and 6. FD-Zn-A and FD-Zn-B are prepared from the same source materials but belong to different freeze drying batches. After measurements of FD-Zn-B, the sample was exposed to an "air+humidity" condition for carrying out a treatment to remove the closed cell structure. FD-Zn-B1 is FD-Zn-B treated in "air+humidity", that is, FD-Zn-B1 corresponds

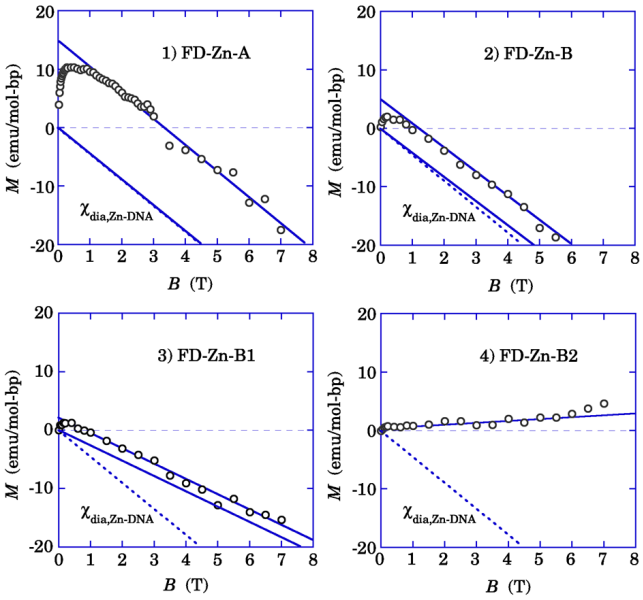

Fig. 6. (Color online) Magnetization curves of FD-Zn-DNA at 300 K, prepared by the treatments described in the text. The solid straight lines in the above panels represent the baseline and the saturation lines of nonlinear magnetization. The dotted line describes the diamagnetism of Zn-DNA.

to the partially hydrated FD-Zn-B. After measurements of FD-Zn-B1 in a sealed quartz tube, FD-Zn-B1 was treated again in "air+humidity" to obtain FD-Zn-B2 as further hydrated FD-Zn-B and measured in a quartz tube. The oxygen contamination below 100 K in the magnetic susceptibility[13] was markedly reduced by the treatments, as shown in Fig. 5.

In addition to oxygen reduction, this treatment generated interesting reproducible changes in the magnetic properties, as demonstrated in Fig. 6:

(1) Suppression of the saturation magnetization M_0, and

(2) Emergence of the temperature-independent linearly increasing paramagnetism χ_{para} with increasing B.

Figure 7 shows the linear, nonsaturating paramagnetic susceptibility of the well-hydrated FD-Zn-B2, which is almost temperature-independent. As the first step to understanding the electronic states of FD-Zn-B2, we assumed the Curie-Weiss formula with one $S = \frac{1}{2}$ spin per base pair,

$$\chi_{\rm CW} = \frac{N_{\rm A} g_e^2 \mu_{\rm B}^2 S(S+1)}{3k_{\rm B}(T+\Theta)}, \tag{1}$$

where $N_{\rm A}$ is the Avogadro constant, g_e the g-factor for a free electron, $\mu_{\rm B}$ the Bohr magneton, and $k_{\rm B}$ the Boltzmann constant. The solid curve in Fig. 7, representing $\chi_{\rm CW}$ with $\Theta \approx 820$ K, is consistent with the magnitude of the observed paramagnetism, but fails to reproduce the

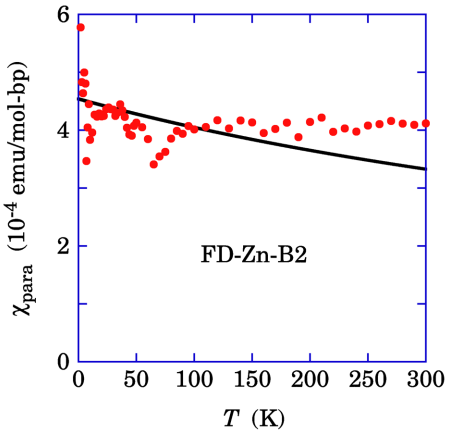

Fig. 7. (Color online) Temperature dependence of the paramagnetic susceptibility $\chi_{\rm para}$ of FD-Zn-B2, which was obtained by subtracting the diamagnetism of Zn-DNA, the oxygen contamination, and the small nonlinear paramagnetism shown in Fig. 6 - 4) from the SQUID susceptibility data. The ambiguity of the estimated $\chi_{\rm para}$ depends on the temperature; below 100 K, the subtraction of the oxygen contribution gives a large ambiguity, but that above 100 K is represented by the data scattering. The solid curve represents the least-squares fit to the Curie-Weiss formula, Eq. (1), which is in poor agreement with the data.

Pauli-like temperature-independent behavior of FD-Zn-B2.

The next possible interpretation is the Pauli susceptibility with $\chi_{\rm Pauli} = N(E_{\rm F})\mu_{\rm B}^2$, where $N(E_{\rm F})$ is the density of states per eV at the Fermi energy. With this relation, the observed $\chi_{\rm para} = 4.0 \times 10^{-4}$ (emu/mol-bp) in Fig. 7 gives 12.4 (states/eV), which indicates that FD-Zn-B2 is a strongly correlated π electron system. With the one-dimensional tight-binding approximation, the π-band width is estimated as $\approx$ 0.05 eV ($E_{\rm F}$ = 25 meV), which is inconsistent with the experimental finding of the temperature-independent susceptibility up to 300 K ($\approx$ 25 meV). Therefore, we assumed that the electronic structure of the hydrated FD-Zn-DNA with the A-form[15,25,29] is three-dimensional (3D). Actually, the exchange interaction of the A-form Mn-DNA is 3D.[15] With the relation $\frac{N(E_{\rm F})}{N} = \frac{3}{2E_{\rm F}}$ for the 3D free-electron model, the band width is estimated as 0.24 eV. This order of the π-band width is common in organic systems, such as molecular conductors and fullerides. Thus, it is reasonably concluded that the hydrated FD-Zn-DNA has a highly correlated π-band with a width of $\approx$ 0.24 eV. This small band width restricts the intraband absorption energy to much less than that of visible light, which is consistent with the transparency of the sample.

In contrast, the completely dehydrated FD-Zn-DNA such as FD-Zn-A carries no $\chi_{\rm Pauli}$, but shows only the nonlinear paramagnetism as a subsidiary property to the freeze drying procedure applied to DNA, as discussed in Sect. 3.1. Thus, FD-Zn-A carries no paramag-

netism originating from the π spin system. It is, however, not probable that the hydrated water molecules in the mechanical treatments cause DNA to create this π spin system. Therefore, this fact suggests that the freeze drying procedure generates the π electron spin system, which loses its magnetism in the dehydrated FD-Zn-DNA, probably because of the strong antiferromagnetic coupling between the neighboring π electron spins. Further discussion will appear in Sect. 3.3.2 with the model for interpreting these observations.

The temperature-independent paramagnetic susceptibility, shown in Fig. 7 is consistent with the ESR intensity reported by Omerzu *et al.*[22] Unfortunately, they could measure the ESR intensity only at the X-band because of the dilute mixture sample of the freeze dried Zn-DNA with excess $ZnCl_2$ and tris-HCl buffer. It is also difficult to extract the temperature-independent paramagnetism using the SQUID magnetometer with the dilute mixture sample. Thus, it is unclear whether they have observed the nonlinear paramagnetism (Figs. 2 and 4) or the Pauli paramagnetism (Fig. 7). The signal intensity of the nonlinear paramagnetism is very strong because of the ferromagnetic enhancement of the local microwave field, which is consistent with the enough strong ESR signal even with their dilute mixture sample. Furthermore, on the basis of the fact that the dehydrated FD-Zn-DNA carries only the nonlinear paramagnetism, it is considered that they observed the nonlinear paramagnetism in the dehydrated FD-Zn-DNA mixture.

3.3.2 Electronic states of FD-Zn-DNA

We propose a model for interpreting the intrinsic magnetic properties of FD-Zn-DNA: the freeze drying procedure generates one $S = \frac{1}{2}$ spin at each base pair, which shows Pauli paramagnetism in the hydrated FD-Zn-DNA but no Pauli paramagnetism in the dehydrated state. The divalent metal ions in the conventional M-DNA synthesized by the ethanol precipitation have usually been hydrated with many water molecules, as shown in Fig. 1. These water molecules prevent the metal ions from forming covalent bonds with the neighboring nitrogen atoms of the bases.[20,26] As a result, the metal ions form the ionic bond with PO_2^- anions of the DNA backbones.

The freeze drying procedure removes water molecules from a frozen aqueous solution, which ideally retains the separation between DNA double helices in the solution. Finally, all the water molecules around the metal ions are removed and then each metal ion is allowed to form preferable configurational bonds with two nitrogen atoms, having a lone electron pair, in place of the imino-hydrogen atom of the guanine or thymine base, as shown in Fig. 8, similarly to metal phthalocyanines. The loss of the imino-hydrogen atom in the guanine or

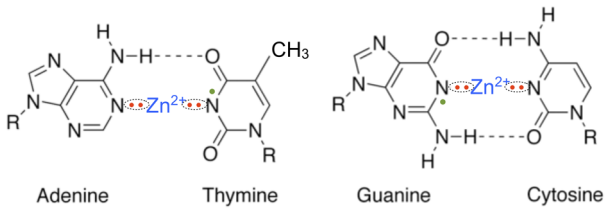

Fig. 8. (Color online) Model for the freeze dried Zn-DNA. All the hydrated water molecules are removed by the freeze drying procedure. Zn ions prefer to form configurational bonds in place of the imino-hydrogen atoms of guanine and thymine bases. As a result, one unpaired electron on the nitrogen atom provides $S = \frac{1}{2}$ spin per base pair.

thymine base changes the number of electrons from even to odd, that is, the creation of an unpaired π electron spin in each base pair of FD-Zn-DNA takes place.

The generated π electron spins should delocalize all over the base pair with the Zn ion to reduce the kinetic energy. The magnetic interaction between the spins of neighboring base pairs separated by approximately 3.4 Å is expected to be antiferromagnetic. The dehydrated FD-Zn-DNA shows only diamagnetism ascribable to that of Zn-DNA, which suggests that the expected paramagnetism of the π electron spins is completely suppressed by the strong antiferromagnetic coupling between the spins of the neighboring base pairs. Thus, the possible electronic states of the dehydrated FD-Zn-DNA at room temperature are some nonmagnetic ground states with a transition temperature much higher than 300 K.

There are several possible nonmagnetic states in the antiferromagnetic quasi-one-dimensional chain, such as antiferromagnetic (AF) and spin density wave (SDW) states with B parallel to the spontaneous magnetization, spin Peierls (SP), charge density wave (CDW), and charge-ordered (CO) states. Since the present sample is in powder form, there is no possibility of AF and SDW states for the candidate nonmagnetic state. The magnetic susceptibility in the nonmagnetic state disappears exponentially below the transition temperature T_C. Then, T_C should be higher than 600 K, twice the observed temperature of 300 K. It is interesting for SP states that the Hubbard antiferromagnetic exchange energy of a hole carrier in the A-form DNA (A-DNA) is estimated as $J = -2t^2/U = -0.05$ eV with the published values for the transfer energy t on the order of 0.25 eV and the on-site Coulomb repulsion U on the order of 2.5 eV for AT-AT and GC-GC pairs.[30] Thus, the SP state appear to be one of the possible models based on the magnitude of the exchange energy for the dehydrated FD-Zn-DNA at 300 K. It should, however, be noted that 1) the present system of the dehydrated FD-Zn-DNA does not have the same electronic structure as that of the calculated A-DNA; for example, the

present estimation of the π-band width is only 0.24 eV and 2) the Peierls instability of the DNA systems concerning on SP and CDW seems to be implausible because of the sizable structural disorder inherent in DNA. The last candidate is the CO state, in which the intersite Coulomb repulsion V is a crucial parameter other than U. From the value of estimated U and V by Starikov,[30] V is comparable to or larger than U in AT-AT and GC-GC pairs, which suggests the strong possibility of the CO state in the dehydrated FD-Zn-DNA. A molecular size more than 15 Å for a base pair of Zn-DNA, which is much larger than the separation of $\approx$ 3.4 Å between the neighboring base pairs would cause the condition $V > U$. Thus, the π electrons prefer an alternate double occupancy instead of every single occupancy, by paying a cost of U in place of V, resulting in the CO state with the repetition (... $0 : -2e : 0 : -2e : 0$ ...).

In the case of the hydrated FD-Zn-DNA, the water molecules play an important role in reducing the intersite Coulomb repulsion of the π electrons, that is, the screening effect by the water molecules surrounding the base pairs, which results in the condition $V < U$ and the Pauli paramagnetic state with the single occupancy in every base pair instead of the double occupancy. Thus, the present model for Zn-DNA treated by the freeze drying procedure successfully describes the intrinsic part of the anomalous magnetic behavior with the screening effect of the water molecules.

4. Conclusions

We unambiguously demonstrated that the freeze drying procedure applied to Zn-DNA generates a π electron spin at each base pair by the formation of the covalent bonds between the Zn ion and the nitrogen atoms of the bases. The magnetic properties of FD-Zn-DNA can be controlled by adjusting the humidity. The intrinsic nature of the π electron spin system generated by the freeze drying procedure is the nonmagnetic charge-ordered ground state with the intersite Coulomb repulsion $V > U$ in the dehydrated FD-Zn-DNA. In contrast, FD-Zn-DNA hydrated by water molecules shows the Pauli paramagnetism of the π-band with a width of $\approx$ 0.24 eV. This marked change with hydration is due to the screening effect of the intersite Coulomb repulsion V between the π electrons of the neighboring base pairs by the water molecules.

Omerzu *et al*. have reported that the freeze dried Zn-DNA has a degenerate electron spin system on the basis of the temperature dependence of ESR intensity.[22] In the present study, we successfully reproduced the temperature-independent paramagnetic susceptibility in the freeze dried Zn-DNA. However, the magnetization saturates below 0.1 T in the dehydrated

state, whereas the Pauli paramagnetism emerges in the hydrated FD-Zn-DNA. Thus, it is uncertain whether they observed the nonlinear paramagnetism or the Pauli paramagnetism, but the nonlinear paramagnetism would be more probable.

The nonlinear paramagnetism appears commonly in the freeze dried B-DNA and Zn-DNA, which suggests that the magnetic impurities in DNA cause it, that is, the nonlinear paramagnetism is a subsidiary effect of the freeze drying procedure regardless the formation of a metal-DNA complex. The saturation magnetization M_0 corresponds to 0.3% of the $S = \frac{1}{2}$ spin or 0.01% of the $S = \frac{5}{2}$ spin per base pair, which is compatible with the possible magnetic impurities in B-DNA. The nonlinear paramagnetism provides a usual ESR signal around $g \approx 2.1$ with the temperature-independent intensity, which contradicts the reported interpretation with the orbital magnetization of the persistent ring current.[11,28] One possible scenario for the nonlinear paramagnetism is super-paramagnetism of magnetic ion clusters: one divalent magnetic ion inserted in a base pair would trigger cluster formation by breaking the hydrogen bonds of the near-neighbor base pairs and by making it preferable for the other divalent magnetic ions to insert into a disconnected base pair and then to form a cluster. It was found that the nonlinear paramagnetism disappears with increasing humidity, suggesting a role of water molecules in reducing the coherence length of the exchange interaction, which is effectively carried out by the water molecules with their inhomogeneous distribution, as suggested by the hyperfine splitting anomaly in Mn-DNA.[20]

Acknowledgments

One of the authors (K.M.) thanks Prof. Naoya Ogata (Ogata Materials Science Lab.) for kindly providing us with salmon sperm DNA for this study. This work was supported by the Joint Studies Program (2004-2006, 2009-2010) of the Institute for Molecular Science.
Thanks are due to the Instrument Center, the Institute for Molecular Science, for assistance in obtaining the low-temperature ESR spectra. This work was also supported by MEXT KAKENHI on Priority Area (17067015) and by JSPS KAKENHI (C) (22540371).

References

1) H.-W. Fink and C. Schenenberger, Nature **398**, 407 (1999).

2) P. J. de Pablo, F. Moreno-Herrero, J. Colchero, J. Gomez Herrero, P. Herrero, A. M. Baro, P. Ordejon, J. M. Soler, and E. Artacho, Phys. Rev. Lett. **85**, 4992 (2000).

3) D. Porath, A. Bezryadin, S. de Vries, and C. Dekker, Nature **403**, 635 (2000).

4) P. Tran, B. Alavi, and G. Gruner, Phys. Rev. Lett. **85**, 1564 (2000).

5) K. Iguchi, J. Phys. Soc. Jpn. **70**, 593 (2001).

6) A. Rakitin, P. Aich, C. Papadopoulos, Y. Kobzar, A. S. Vedeneev, J. S. Lee, and J. M. Xu, Phys. Rev. Lett. **86**, 3670 (2001).

7) A. Y. Kasumov, M. Kociak, S. Gueron, B. Reulet, V. T. Volkov, D. V. Klinov, and H. Bouchiat, Science **291**, 280 (2001).

8) Y. Zhang, R. H. Austin, J. Kraeft, E. C. Cox, and N. P. Ong, Phys. Rev. Lett. **89**, 198102 (2002).

9) H. Kino, M. Tateno, M. Boero, J. A. Torres, T. Ohno, K. Terakura, and H. Fukuyama, J. Phys. Soc. Jpn. **73**, 2089 (2004).

10) K. Mizoguchi, S. Tanaka, T. Ogawa, N. Shiobara, and H. Sakamoto, Phys. Rev. B **72**, 033106 (2005).

11) S. Nakamae, M. Cazayous, A. Sacuto, P. Monod, and H. Bouchiat, Phys. Rev. Lett. **94**, 248102 (2005).

12) J. B. MacNaughton, M. V. Yablonskikh, A. H. Hunt, E. Z. Kurmaev, J. S. Lee, S. D. Wettig, and A. Moewes, Phys. Rev. B **74**, 125101 (2006).

13) K. Mizoguchi, S. Tanaka, and H. Sakamoto, Phys. Rev. Lett. **96**, 089801 (2006).

14) S. Nakamae, M. Cazayous, A. Sacuto, P. Monod, and H. Bouchiat, Phys. Rev. Lett. **96**, 089802 (2006).

15) K. Mizoguchi, S. Tanaka, M. Ojima, S. Sano, M. Nagatori, H. Sakamoto, Y. Yonezawa, Y. Aoki, H. Sato, K. Furukawa, and T. Nakamura, J. Phys. Soc. Jpn. **76**, 043801 (2007).

16) S. S. Mallajosyula and S. K. Pati, Phys. Rev. Lett. **98**, 136601 (2007).

17) R. G. Endres, D. L. Cox, and R. R. P. Singh, Rev. Mod. Phys. **76**, 195 (2004).

18) J. S. Lee, L. J. P. Latimer, and R. S. Reid, Biochem. Cell Biol. **71**, 162 (1993).

19) A. Omerzu, D. Mihailovic, B. Anzelak, and I. Turel, Phys. Rev. B **75**, 121103R (2007).

20) M. Nagatori, M. Ojima, Y. Ibuki, H. Sakamoto, and K. Mizoguchi, J. Phys. Soc. Jpn. **80**, 114803 (2011).

21) M. Tsuburaya, H. Sakamoto, and K. Mizoguchi, Phys. Rev. E **89**, 022719 (2014).

22) A. Omerzu, B. Anzelak, I. Turel, J. Strancar, A. Potocnik, D. Arcon, I. Arcon, D. Mihailovic, and H. Matsui, Phys. Rev. Lett. **104**, 156804 (2010).

23) K. Mizoguchi, S. Tanaka, and H. Sakamoto, J. Low Temp. Phys. **142**, 379 (2007).

24) K. Mizoguchi, Proc. SPIE **7040**, 70400Q (2008).

25) K. Mizoguchi, Proc. SPIE **7765**, 77650R (2010).

26) K. Mizoguchi, Proc. SPIE **8103**, 810307 (2011).

27) M. S. Blois Jr., J. E. Maling, and L. T. Taskovich, Biophys. J. **3**, 275 (1963).

28) C. H. Lee, Y.-W. Kwon, E.-D. Do, D.-H. Choi, J.-I. Jin, D.-K. Oh, and J. Kim, Phys. Rev. B **73**, 224417 (2006).

29) R. P. Bowater, *Nature Encyclopedia of the Human Genome,* ed. D. M. Cooper (Macmillan, London, 2003) Vol. 1, p. 1.

30) E. B. Starikov, Philos. Mag. Lett. **83**, 699 (2003).